VIBRO-ACOUSTIC MODELING OF SANDWICH AND UNRIBBED OR RIBBED PANELS WITH THICK LAMINATE COMPOSITE SKIN USING STATISTICAL ENERGY ANALYSIS

Abderrazak Mejdi[1], Bryce Gardner[1] and Chadwyck Musser[1]

[1]ESI Group US R&D, 12555 High Bluff Dr. Suite 175, San Diego, California, 92130, USA
Email: amj@esi-group.com

ABSTRACT

This paper investigates the vibro-acoustic response of stiffened and unstiffened laminate composite structures and sandwich structures based on a Statistical Energy Analysis (SEA) approach. SEA is a modeling procedure which uses energy flow relationships for the theoretical estimation of the dynamic response as well as the sound transmission through structures in resonant motion. The accuracy of SEA is related to the accurate estimates of its parameters (modal density, Damping Loss Factor (DLF) and the Coupling Loss Factor (CLF)). Wave and modal based approaches are developed to predict the SEA parameters for both stiffened and unstiffened composite panels and sandwich panels. For composite structures each layer is assumed to be a thick laminate with orthotropic orientation. Moreover, rotational inertia and transversal shearing, membrane and bending deformations are accounted for. First order shear deformation theory is used. The developed approach handles symmetrical and asymmetrical constructions of an unlimited number of transversal incompressible layers. Moreover, for the case of a ribbed panel with thick composite skin, the effect of variable spacing of the ribs is accounted for. The sandwich model uses a discrete displacement field for each layer and allows for out-of-plane displacements and shearing rotations. The accuracy of this modeling approach is confirmed through comparison to measured test data and alternate validated theoretical results. The advantages of the new developed models compared to the classical models are also investigated. Representative examples of aircraft interior noise predictions for typical load cases are shown and the use of SEA models as a tool for guiding construction of multi-layer lightweight structures to meet acoustic performance and weight targets and optimize designs are presented. Conclusions about the overall applications and improvements offered by these approaches, current limitations, and future work to extend and improve these approaches are given.

1 INTRODUCTION

Nowadays there is an increasing use of sandwich and laminate composite panels due to their light weight and higher stiffness. The ability to accurately predict the dynamic structural properties of such structures is essential in order to accurately predict the corresponding interior noise and structural vibration levels for many industrial applications including aerospace vehicles. Unlike the vibro-acoustic response of simple continuous structures, a detailed analysis of wave motions for stiffened plates is often difficult to achieve because of the complexity of the structural configuration and the uncertainty of the boundary conditions. Most of the previous research focused on the modelling of ribbed panels with regular spacing between stiffeners [1]-[2]. In practice ribbed panel construction is always accompanied with non-uniform, statistically variable spacing between stiffeners even when uniform spacing is intended. Little previous research was developed to account for this stiffener spacing uncertainty.

The Statistical Energy Analysis (SEA) technique is commonly used at higher frequencies to predict airborne and structure borne noise transmission for many industrial applications. Being able to properly characterize complex ribbed and unribbed multi-layer lightweight structures and derive the modal density and coupling loss factors (CLF) is essential. A large number of researchers have studied these parameters for single-layer structures but only a limited amount of work has been carried out to determine these parameters for sandwich panel and ribbed or unribbed panels with thick composite skin. For instance, Zhou and Crocker [3] analysed the sound transmission of sandwich panels where the classical sandwich formulation is used to predict the modal density and the coupling loss factor is measured. Other researchers modelled the laminate composite as a two-dimensional problem wherein the displacement field in each lamina is based on Kirchhoff’s hypothesis [4]-[6]. Moreover, most of the existing models neglect the shear and the inplane contributions as well as the rotational inertia that strongly influence the high-frequency behavior of these structures. More accurate results are provided by a first-order shear deformation theory [7]-[9] or other higher order shear deformation theories [10]. The first-order shear deformation theory based on Reissner–Mindlin-type assumptions takes the transverse shear deformation into account. However, it requires shear correction factors to compensate for errors resulting from the approximation of the shear-strain distribution. For instance, Ghinet and Atalla [11]-[12] used Reissner–Mindlin-type assumptions in a Transfer Matrix Method (TMM) context. For ribbed panels, the stiffener spacing uncertainty effect was always ignored in the modelling of these structures. Only a few researchers studied this effect; for instance, Mejdi and Atalla [13] developed a semi analytical model to analyses ribbed panels with evenly and unevenly stiffened composite laminate flat structure. Langley [14] derived the modal density of periodically stiffened beam and plate structures in terms of phase constants, which were associated with propagating wave motion. In his analysis he assumes that the modal density is not affected by the imperfection in the attachment.

In this paper, a wave and modal based approach are developed to model both sandwich and ribbed or unribbed panels with thick composite skins in an SEA context. The effect of shear deformation and the in-plane / bending coupling effects are employed to improve the vibro-acoustic response prediction of multilayer structures. Moreover, for ribbed panels, the stiffeners spacing uncertainty effect is accounted for. SEA prediction using classical models are compared to the presented models using thick plate theory. The latter are found more suitable for both low- and high- frequency analysis. The stiffeners spacing uncertainty has an important effect on the dynamic response of ribbed panels.

2 THEORY

2.1 Thick composite model

The laminate panels considered here have a symmetric or an asymmetric configuration. The panel is assumed infinite. For a point M belonging to the laminated composite shell, the displacement field is defined by the Mindlin type assumption where both bending and transverse shear effects are considered:

$$\begin{aligned} U(x,y,z) &= U_0(x,y) + z\varphi_x(x,y) \\ V(x,y,z) &= V_0(x,y) + z\varphi_y(x,y) \\ W(x,y,z) &= W_0(x,y) \end{aligned} \tag{1}$$

U, V and W are the in-plane and the transversal displacements and φ_x, φ_y are the rotational displacements in *x* and *y* directions, respectively and z is the layer's point position from lamina mid-plane. Geometrically, the shell is considered to be of infinite extent in the axial (*x*) direction and thus the origin for both *x* and *y* is arbitrary. Nevertheless, the origin for the *z* axis is defined on a reference surface passing through the middle thickness of the shell.

The dynamic equilibrium relations of the unstiffened in-vacuum panel are given by integrating the stress continuity relation through the thickness of the lamina [13]:

$$\begin{aligned} &\frac{\partial N_x}{\partial x} + \frac{\partial N_{xy}}{\partial y} = (m_s)\frac{\partial^2 U}{\partial t^2} + (I_{z2})\frac{\partial^2 \varphi_x}{\partial t^2} \\ &\frac{\partial N_y}{\partial y} + \frac{\partial N_{xy}}{\partial x} = (m_s)\frac{\partial^2 V}{\partial t^2} + (I_{z2})\frac{\partial^2 \varphi_y}{\partial t^2} \\ &\frac{\partial Q_x}{\partial x} + \frac{\partial Q_y}{\partial y} = (m_s)\frac{\partial^2 W}{\partial t^2} \\ &\frac{\partial M_x}{\partial x} + \frac{\partial M_{xy}}{\partial y} - Q_x = I_z\left(\frac{\partial^2 \varphi_x}{\partial t^2}\right) + I_{z_2}\left(\frac{\partial^2 U}{\partial t^2}\right) \\ &\frac{\partial M_y}{\partial y} + \frac{\partial M_{xy}}{\partial x} - Q_y = I_z\left(\frac{\partial^2 \varphi_y}{\partial t^2}\right) + I_{z_2}\left(\frac{\partial^2 V}{\partial t^2}\right) \end{aligned} \tag{2}$$

where N_x, N_y, N_{xy} are the in plane forces and M_x, M_y, M_{xy} are the bending moments and Q_x, Q_y are the shearing forces. m_s and I_z, I_{z2} are the total mass per unit area and the total rotational inertia terms, respectively. Using the stress displacement relation and integrating the stress through the thickness, the constitutive relation between the forces and the displacements can be written as:

$$\begin{bmatrix} N_x \\ N_y \\ N_{xy} \\ M_x \\ M_y \\ M_{xy} \\ Q_x \\ Q_y \end{bmatrix} = \begin{bmatrix} A_{11} & A_{12} & A_{16} & B_{11} & B_{12} & B_{16} & 0 & 0 \\ A_{12} & A_{22} & A_{26} & B_{12} & B_{22} & B_{26} & 0 & 0 \\ A_{16} & A_{16} & A_{66} & B_{16} & B_{26} & B_{66} & 0 & 0 \\ B_{11} & B_{12} & B_{16} & D_{11} & D_{12} & D_{16} & 0 & 0 \\ B_{12} & B_{22} & B_{26} & D_{12} & D_{22} & D_{26} & 0 & 0 \\ B_{16} & B_{26} & B_{66} & D_{16} & D_{26} & D_{66} & 0 & 0 \\ 0 & 0 & 0 & 0 & 0 & 0 & F_{44} & F_{45} \\ 0 & 0 & 0 & 0 & 0 & 0 & F_{45} & F_{55} \end{bmatrix} \begin{bmatrix} \partial U/\partial x \\ \partial V/\partial y \\ \partial U/\partial y + \partial V/\partial x \\ \partial \varphi_x/\partial x \\ \partial \varphi_y/\partial y \\ \partial \varphi_x/\partial x + \partial \varphi_y/\partial y \\ \partial W/\partial x + \partial \varphi_x/\partial x \\ \partial W/\partial y + \partial \varphi_y/\partial y \end{bmatrix} \tag{3}$$

where A_{ij}, B_{ij} and D_{ij} are the extensional, extensional-bending and bending stiffness. The equations of motion can be obtained by introducing (3) into (2) and assuming a solution in the following form:

$$\{e\} = \{U, V, W, \varphi_x, \varphi_y\}^T \exp\left(jk_x + jk_y + j\omega t\right) \tag{3}$$

where k_x and k_y are the components of the structural wave number, k_p is defined as a function of the heading angle θ:

$$\begin{aligned} k_x &= k_p \cos(\theta) \\ k_y &= k_p \sin(\theta) \end{aligned}, \tag{4}$$

Using Eqs. (2)-(4), we obtain the following compact matrix equation:

$$\left\{k_p^2\left[A_3\right]-ik_p\left[A_2\right]-\left[A_1\right]-\omega^2\left[M\right]\right\}\left\{e\right\}=0\,, \tag{5}$$

For a wave-based approach, one can obtain the eigen solutions from Eq (6). The three smallest real positive solutions correspond to the bending, extension and shearing wavenumbers. The extensional and bending matrices can be obtained from the eigen solution and all the SEA parameters: CLF, DLF and modal density, can be obtained.

2.2 Ribbed panel with thick composite skin and periodic and variable stiffener spacing

2.2.1 Periodic ribbed panels

For ribbed panel, the stiffened effect could be accounted for by correcting the mass and stiffeners in the wavenumber domain. Indeed, Bremner [16] has explained the distinct behaviours in terms of wavenumbers of a flat ribbed plate of width L_x and height L_y stiffened with ribs and frames with spacing S_x and S_y between the ribs and frames. As the modal half-wavelength in the *x* and *y* directions goes below the L_x and L_y dimensions, the plate behaviour shifts from global behaviour, over the plate area (L_x, L_y), to periodic behaviour over areas delimited by (S_x, L_y), (L_x, S_y). Finally, when the modal half-wavelength goes below the rib and frame spacing S_x and S_y, the modal behaviour is determined by the behaviour of a flat uniform subpanel delimited by the ribs and frames (local behaviour). Those four conditions represent the four models required when fully describing the modal behaviour of a stiffened plate over a large frequency band. When a particular condition is met for periodic modes behaviour, the number of modes should be multiplied by the multiplicity factor μ.

For example, the mass and stiffness correction in region 1 where the bending wave numbers $k_m < \pi/S_x$ and $k_n < \pi/S_y$ and both *x* and *y* ribs smeared over surface (L_x , L_y) with a group of multiplicity $\mu_p = 1$, are given by:

$$m^{total} = m^{skin} + \frac{m_{bx}}{S_x} + \frac{m_{by}}{S_y}$$

$$D_{11} = D_{11}^{skin} + \frac{(EI_{bx})}{S_x} + \frac{z^2(EA_x)}{S_x}; D_{22} = D_{22}^{skin} + \frac{(EI_{by})}{S_y} + \frac{z^2(EA_y)}{S_y}; D_{33} = D_{33}^{skin} + 0.25\frac{(G_x J_{bx})}{S_x} + 0.25\frac{(G_y J_{by})}{S_y}$$

$$A_{11} = A_{11}^{skin} + \frac{(EA_{bx})}{S_x}; A_{22} = A_{22}^{skin} + \frac{(EA_{by})}{S_y}; A_{33} = A_{33}^{skin} + \frac{(k_x G_x A_{bx})}{4S_x} + \frac{(k_y G_y A_{by})}{4S_y};$$

$$B_{11} = B_{11}^{skin} + \frac{z(EA_{bx})}{S_x}; B_{22} = B_{22}^{skin} + \frac{z(EA_{by})}{S_y}; B_{33} = B_{33}^{skin} + \frac{z(k_x G_x A_{bx})}{4S_x} + \frac{z(k_y G_y A_{by})}{4S_y}$$

$$F_{44} = F_{44}^{skin} + \frac{(k_x G_x A_{bx})}{S_x}; F_{55} = F_{55}^{skin} + \frac{(k_y G_y A_{by})}{S_y} \tag{7}$$

Where *m* denote the mass, *E, G* are the stiffener's young and shear modulus respectively, *I* and *A* are the stiffener's moment of intertie and cross section respectively.

Once the mass and stiffness are corrected, the modal frequency can be obtained by considering a simply-supported boundary condition and by solving Eq (6) for each mode order. Indeed, for a simply-supported boundary condition, the bending wavenumber is given by $k_{mn} = \sqrt{\left(m\pi/L_x\right)+\left(n\pi/L_y\right)}$ where *m* and *n* are the modal orders. Eq (6) can be rewritten as:

$$\left\{k_{mn}^2\left[A_3\right]-ik_{mn}\left[A_2\right]-\left[A_1\right]-\omega_{mn}^2\left[M\right]\right\}\left\{e\right\}=0 \tag{8}$$

To account for any curvature and tension effects that may be acting on the structure, the modal frequency can be corrected as:

$$\omega_{mn\_cor} = \omega_{mn} + C + T \tag{9}$$

where the terms C and T are the curvature and tension correction factors.

By solving Eq (8) for the modal frequency, the mode list can be obtained by evaluating the modal frequency regarding each bandwidth and in this manner all the SEA parameters can be obtained.

2.2.2 Variable spacing effect

To account for the uncertainties in the ribs spacing, a statistical process can be employed by considering an ensemble of *i* spacing varying by a certain percentage over the nominal rib spacing values. It is assumed that the spacing uncertainty can be computed as though it has a normal distribution as shown in Figure 1:

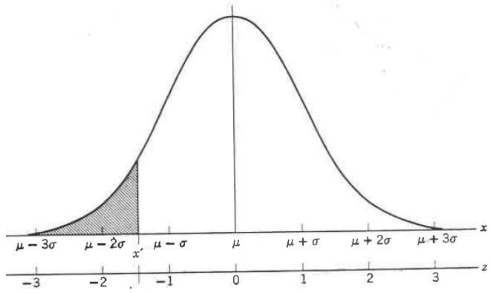

Figure 1: Graph of normal probability density function.

$$f = \frac{1}{\sqrt{2\pi}} e^{\frac{-z^2}{2}} \quad \text{where} \quad z=[-3\ -2\ -1\ 0\ 1\ 2\ 3] \tag{10}$$

where f is the probability density function (pdf). The modal energy corresponding to each spacing could be computed using the power balance equation:

$$\pi_i = \omega\left[\eta\left(S_x^i, S_x^j\right)\right]E_i \Leftrightarrow E_i = \omega\left[\eta\left(S_x^i, S_x^j\right)\right]^{-1}\pi_i \ \text{ where } i = 1, 2, ..7 \tag{11}$$

$\eta(S_x^i, S_y^i)]$ is the SEA coupling matrix corresponding to a given spacing S_x^i, S_y^i . E_i and π_i are the corresponding modal energy and injected power respectively.

The average estimate of all the SEA parameters and vibro-acoustic responses can be obtained using the following formulation:

$$\langle \mathrm{V} \rangle = \sum_{i=1}^{7} \alpha_i V_i \quad \text{where} \quad \alpha_i = \frac{f^i}{\sum_{i=1}^{7} f^i} \tag{12}$$

V_i is an SEA parameter such as the modal density, CLF, DLF or injected power and f^i is the pdf given by $f^i = \frac{1}{\sqrt{2\pi}} e^{-z_i^2/2}$ for a given $z_i = [-3 - 2 - 1\ 0\ 1\ 2\ 3]$ as mentioned in Eq (10).

2.3 Sandwich model with composite skin

For a sandwich model, a Mindlin-type assumption is used to describe the displacement field of the core [12]. The skins are assumed to be thinner than the core and display bending behaviour. Their displacement field is built using the Love-Kirchhoff's assumptions but is corrected to account for the rotational influence of the transversal shearing in the core [12].

$$\begin{cases} u^k(x,y,z) = u_0^k(x,y) - z\dfrac{\partial w}{\partial x}(x,y) + r_{kx} \\ v^k(x,y,z) = v_0^k(x,y) - z\dfrac{\partial w}{\partial y}(x,y) + r_{ky} \ ; \ k = 1;3 \\ w^k(x,y,z) = w(x,y) \end{cases} \tag{13}$$

where r_{kx} and r_{ky} are the rotational coefficients.

Perfect bonding of the layers is assumed, so that the displacement field remains continuous throughout the interface between two consecutive layers.

The relations of stresses' dynamic equilibrium are written for each layer separately in order to develop the continuity of stress relations at the interface between the layers. These relationships are next integrated through the layer's thickness and the dynamic equilibrium relations along the *x* and *y* directions are obtained. For the top skin – core interface represented by the superscript ^{1}, the relations of continuity are written as follows:

$$\begin{aligned} &\frac{\partial N_x^1}{\partial x} + \frac{\partial N_{xy}^1}{\partial y} - \tau_{xx}^1 - (I_{z1}^1 \frac{\partial w}{\partial x} - I_{z2}^1 \varphi_x) = 0 \\ &\frac{\partial N_y^1}{\partial y} + \frac{\partial N_{xy}^1}{\partial x} - \tau_{yz}^1 - (I_{z1}^1 \frac{\partial w}{\partial x} - I_{z2}^1 \varphi_x) = 0 \end{aligned} \tag{14}$$

The panel's dynamic behaviour is governed by the dynamic equilibrium relations of the forces and moments along the *x*, *y* and *z* directions. The sandwich-type panel assumptions are considered; the membrane forces N_x, N_y and N_{xy} and the bending moments M_x, M_y and M_{xy} are computed through the thickness of the skins while the transversal shearing forces Q_x and Q_y are expressed through the core's thickness. Considering the stresses' continuity relations along the *x*, *y*, and *z* directions as well as the panel's incompressibility along the *z* direction and integrating through the panel thickness, the following equilibrium relations can be written:

$$\begin{aligned} &\frac{\partial Q_x}{\partial x} + \frac{\partial Q_y}{\partial y} = m_s \frac{\partial^2 W}{\partial t^2} \\ &\frac{\partial M_x}{\partial x} + \frac{\partial M_{xy}}{\partial y} - Q_x = I_{z\_t}\left(\frac{\partial^2 U}{\partial t^2}\right) \\ &\frac{\partial M_y}{\partial y} + \frac{\partial M_{xy}}{\partial x} - Q_y = I_{z\_t}\left(\frac{\partial^2 V}{\partial t^2}\right) \end{aligned} \tag{15}$$

The shearing forces Q_x and Q_y can be replaced in the last two equations to express the following relationship of motion:

$$\begin{aligned} &\frac{\partial^2 M_x}{\partial x^2} + 2\frac{\partial^2 M_{xy}}{\partial x \partial y} + \frac{\partial^2 M_y}{\partial y^2} - \\ &I_{z_2}\left(\frac{\partial^2 U}{\partial t^2}\right) - I_{z_2}\left(\frac{\partial^2 V}{\partial t^2}\right) + (m_s)\frac{\partial^2 W}{\partial t^2} = 0 \end{aligned} \tag{16}$$

The stresses' continuity relations compose the system of dynamic equilibrium equations of sandwich composite panels. This system can be expressed in a matrix form using the constitutive equation Eq (4) in the same solution form as in Eq (6):

$$\left\{k^4[A] + jk^3[B] + k^3[C] + jk[D] + [E]\right\}\{e\} = 0 \tag{17}$$

As for the thick composite model, the eigenvalue problem can be solved and sorted out to find the three smallest real positive solutions. All the SEA parameters (CLF, DLF and modal density) can then be easily computed.

3 NUMERICAL RESULTS

Various numerical examples are given and validated by the VA One commercial software code. Both ribbed and unribbed panels with thick composite and uniform skin are analyzed. The effect of variable spacing between stiffeners reinforcing thick composite skin is also analysed. The accuracy of the modeling approach for sandwich panels in which the skin layers are made of composite materials is also analysed. In the following examples, both the wave and modal approach based predictions using the different models are examined by comparing various vibro-acoustic indicators with experimental and existing models. Acoustic behavior under airborne and structure borne excitation is investigated. VA One capabilities and accuracy of the sound transmission prediction of various types of structures are checked by analyzing their effects.

3.1 Thick versus thin composite model

A representative model of helicopter with skin made up of ribbed panel with composite skin (Figure 2-a) is investigated in the following example. The skin is made up of three layers of Graphite/Epoxy. Each layer of the composite is 2.5mm thick. Both thick and thin shell theories are employed to predict the sound transmission loss (STL) between the cockpit and the cabin which are separated by the bulkhead which is an unstiffened composite shell having the same properties as the ribbed panel's skin. The structural wavenumber of the bulkhead is also predicted using both thick and thin shell theories. It is observed in Figure 2-b that the bulkhead has pure bending behaviour at low frequencies and pure shearing behaviour at high frequencies. In fact, the two theories give approximately the same STL until 1kHz. However, the latter is overestimated using the classical thin plate theory over 1kHz as shown in Figure 2- c. This is mainly due to the fact the the shear deformation effect is ignored in thin shell theory. Also, the in-plane and out-of-plane coupling effect is ignored in the thin shell theory. The effects are usually negligible at low frequencies but must be included to model the physics of the structure at higher frequencies.

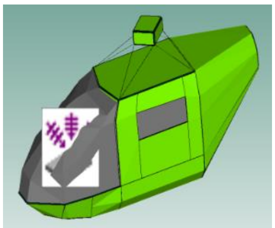

a) Representative helicopter model.

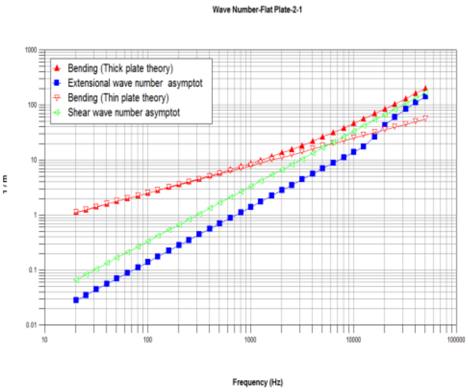

b) predicted wavenumber for unstiffened bulkhead example panel using thick and thin composite models

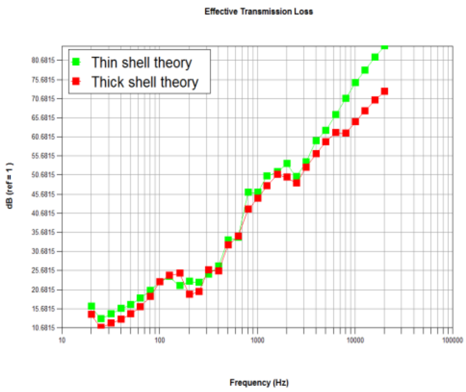

c) Comparison between predicted transmission loss using thick and thin composite models with reference [15]

Figure 2: predicted wave number and transmission loss of unstiffened bulkhead example panel using thick and thin shell theory.

3.2 Ribbed panel with thick composite skin and variable spacing

In order to analyze the variable spacing effect, a cylindrical shell with skin made up of 3 mm steel material is considered. The cylindrical skin is reinforced by eight stiffeners. The modal density is predicted for both evenly and unevenly spaced stiffeners. To account for the uncertainties in the rib spacing, a statistical process has been evolved by considering an ensemble of 7 spacing varying by 5% over the nominal values. It is observed that, the averaged estimation smoothens out the modal density curve, which is in very good agreement with experimental data compared to reference [17] and regular spacing prediction which show distinct, large peaks and valleys at certain frequencies for a periodic stiffened panel. This is mainly due to the periodicity characteristic of the panel. Indeed, in the case of periodic spacing with uniform spacing, all the stiffeners behave as pass band filter at the same frequencies, thus the energy is totally transmitted between sub panels. However, for uneven stiffener spacing, some of the stiffeners behave as pass band filter while others behave as stop band filter and so the modal density results are averaged out more evenly in frequency as a result as can be seen in Figure 3.

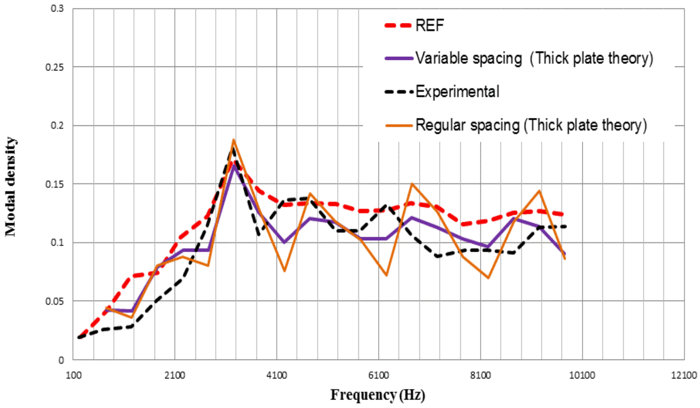

Figure 3: Comparison of ribbed panel modal density with even and uneven stiffener spacing versus experimental and Reference [17].

3.3 Sandwich model

In the following example, the accuracy of the sandwich model is examined by comparison with experimental results. A sandwich with honeycomb core and isotropic face with Density ρ =1716 (kg/m^3), Young's modulus E=49 GPa, poisons ratio $\nu = 0.134$ and thickness hs=5.84x10^{-4} m. Experimental data is shown compared to a prediction using classical theory with thin plate assumptions versus the new approach using thick plate theory (Figure 4). Excellent agreement is found versus the experimental results when using the presented sandwich model. However, the classical sandwich model fails to correctly capture the physical behavior. Indeed, the SEA estimates provide unreasonable predictions for the sound transmission loss using the classical sandwich model at and over the coincidence frequency region which is predicted to occur about 300 Hz lower in frequency than the measurement. The prediction making use of the presented sandwich model does capture the correct coincidence frequency region in comparison to the measured data.

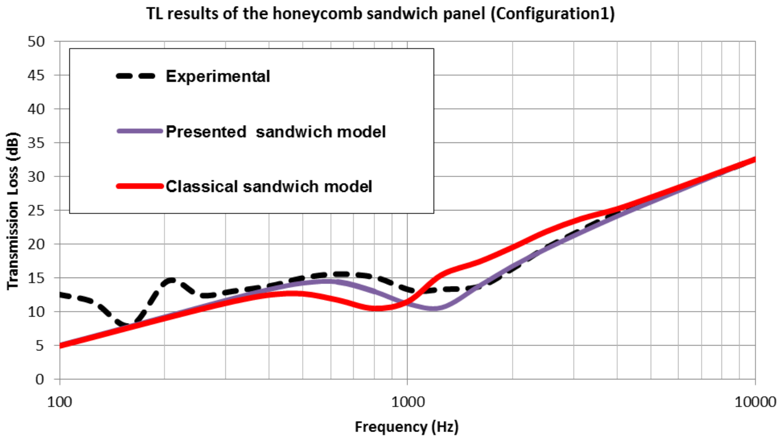

Figure 4: Comparison between predicted transmission loss using improved sandwich model and experimental result.

3.4 Material properties' effect

In the following example, the structure borne excitation from the helicopter gearbox is simulated in VA One as a velocity constraint applied to the bottom face of the gear box (Figure 5-a). This excitation is transmitted to the helicopter skin through eight rectangular metallic beams. The pressure level inside the cockpit is predicted for two different configurations. In the first configuration, the bulkhead wall separating the cockpit and the cabin is modeled as 3mm aluminum structure. In the second configuration, the bulkhead is modeled as sandwich with two 3mm aluminum skins and a 6.35 mm honeycomb core. The rest of the helicopter skin is made up of ribbed panels with composite skin made up of three layers of Graphite/Epoxy of 1 mm thickness each. It is observed that the pressure inside the cockpit has different level for the two configurations below the ring frequency at 200 Hz thought to be the ring frequency of the whole cockpit curved shell while between the ring frequency and the critical frequency at 3 kHz, the two configurations have also different level. This is mainly due to the fact that the sandwich has a pure bending behavior of the panel at low frequencies and core's shearing at mid frequencies as shown in the wave number plot in figure 5-b. The interior SPL levels are shown in Figure 5-c where it can be seen that above the critical frequency the sandwich and the aluminum bulkhead have the same pressure level. This is due to the fact that at high frequencies, the sandwich is controlled by a decoupled skin bending effect which has the same properties as the uniform panel as shown in figure 5-b.

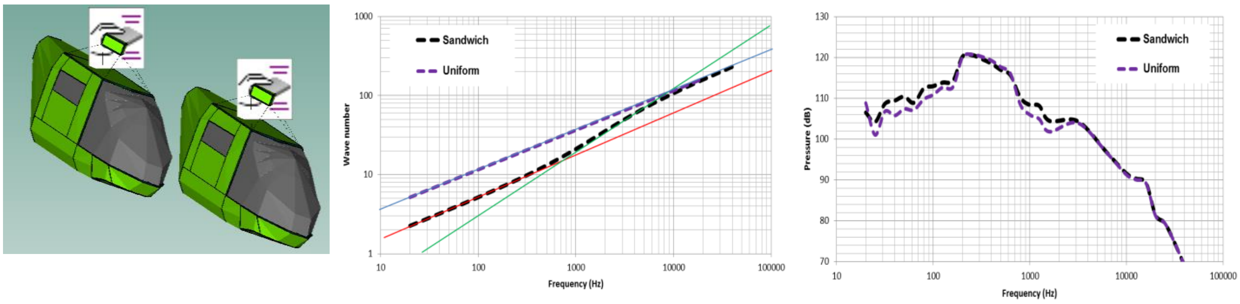

a) Representative helicopter model.

b) Wavenumber comparison on sandwich and uniform bulkhead panels

c) Comparison of pressure level in the cockpit for two different bulkhead configurations

Figure 5: Wavenumber of bulkhead panels and pressure level in the cockpit due to structure born excitation

4 CONCLUSION

In this paper, a model for sandwich panel with composite face sheets for both ribbed and unribbed cases is developed. The ribbed panels' skin is assumed to be thick composite and the stiffeners may be modeled as unevenly spaced. The theories are developed in a wave and modal approach context. For the thick composite model, shear deformation and in-plane / out-of-plane motion coupling were both taken into account. For the sandwich model, the physical behavior of the panel is represented using a discrete lamina description. The acoustic transmission problem is represented within the SEA context and is successfully compared to experiments and to existing models. The SEA estimate provides reasonable results at low frequencies using the classical composite and classical sandwich models. However, they both fail to correctly capture the physical behavior at mid and high frequencies and the thick plate theory is needed to capture these high-frequency effects. The interior noise effect due to airborne and structure borne excitations were analysed and the effect of material properties was also investigated. It was found that the interior noise level is sensitive to the material properties and the excitation type. This work can be extended to model the ribbed panel stiffeners as composite material. The application of sandwich as a skin for ribbed panel constitutes another challenge.

REFERENCES

[1] A. Mejdi and N. Atalla, Dynamic and acoustic response of bidirectionally stiffened panels with eccentric stiffeners subject to airborne and structureborne excitations, *J. Sound. Vib*. 329(21), 4422–4439 (2010).

[2] Abderrazak Mejdi, Julien Legault and Noureddine Atalla, Transmission loss of periodically stiffened laminate composite panels: Shear deformation and in-plane interaction effects. *J. Acoust. Soc. Am*. 131 , 174 (2012)

[3] Ran Zhou , Malcolm J.Crocker , Sound transmission loss of foam-filled honeycomb sandwich panels using statistical energy analysis and theoretical and measured dynamic properties. *J. Sound. Vib*. 329 (2010) 673–686.

[4] R.S. Langley, The modal density and mode count of the thin cylinders and curved panels, *J. Sound. Vib* 169 (1994).

[5] Roussos L. A., Powell C. A., Grosveld F. W. and Koval L. R,. Noise Transmission Characteristics of advanced composite structural materials, *J. Aircraft*, vol. 21, no.7, 528-535, (1984).

[6] J. P. D. Wilkinson, Modal densities of certain shallow structural elements, *J. Acoust. Soc. Am.*, Vol. 43, No. 2, 245-251, 1968.

[7] Mindlin RD. Influence of rotatory inertia and shear on flexural motions of isotropic, elastic plates. *ASME J Appl Mech* 1951:1831–8.

[8] Nosier A, Kapania RK. Free vibration analysis of laminated plates using a layer-wise theory. In: *AIAA/ASME/ASCE/AHS/ASC structures, structural dynamics, and materials conference no. 34, La Jolla, CA, ETATS-UNIS*, vol. 31 (12); 1993. p. 2335–46.

[9] Michael P. Nemeth, A Treatise on Equivalent-Plate Stiffnesses for Stiffened Laminated-Composite Plates and Plate-Like Lattices, *Langley Research Center, Hampton, Virginia, NASA/TP*-2011-216882

[10] Reddy JN. A simple higher-order theory for laminated composite plates. *ASME J Appl Mech* 1984;51(4):745–52.

[11] Ghinet S, Atalla N. Diffuse field transmission into infinite sandwich composite and laminate composite cylinders. *J Sound Vib* 2006;289(4–5):745–78.

[12] Ghinet S, Atalla N. Vibro-acoustic behaviours of flat sandwich composite panels. *Trans Can Soc Mech Eng* 2006;30(4):473–93.

[13] A. Mejdi and N. Atalla, Vibroacoustic analysis of laminated composite panels stiffened by complex laminated composite stiffeners, *International Journal of Mechanical Sciences* 58 (2012) 13–26

[14] R.S. Langely, On the modal density and energy flow characteristics of periodic structures, *J. Sound. Vib* 172 (1994) 491–511.

[15] Shorter P. J., Wave propagation and damping in linear viscoelastic laminates, *J. Acoust. Soc. Am.*, 115(5), 1917–1925, (2004).

[16] P.G. Bremner, Vibro-acoustics of ribbed structures – a compact modal formulation for SEA models, *Noise-Con* 94, Ft. Lauderdale, Florida (1994).

[17] P. Ramachandran, S. Narayanan, Evaluation of modal density, radiation efficiency and acoustic response of longitudinally stiffened cylindrical shell, *J. Sound. Vib* 304 (2007) 154–174